Cationic Amphiphiles Increase Activity of Aminoglycoside Antibiotic Tobramycin in the Presence of Airway Polyelectrolytes

ARTICLE *in* JOURNAL OF THE AMERICAN CHEMICAL SOCIETY · JANUARY 2009

Impact Factor: 12.11 · DOI: 10.1021/ja803925n · Source: PubMed

J|A|C|S ARTICLES

Published on Web 12/11/2008

Cationic Amphiphiles Increase Activity of Aminoglycoside Antibiotic Tobramycin in the Presence of Airway Polyelectrolytes

Kirstin R. Purdy Drew,[†,⊥,▽] Lori K. Sanders,[†] Zachary W. Culumber,[‡] Olena Zribi,[§] and Gerard C. L. Wong*[,†,§,∥]

Departments of Materials Science and Engineering, Animal Biology, Physics, and Bioengineering, University of Illinois at Urbana−Champaign, Urbana, Illinois 61801

Received May 25, 2008; E-mail: gclwong@illinois.edu.

Abstract: It is empirically known that anionic polyelectrolytes present in cystic fibrosis (CF) airways due to bacterial infection significantly decrease the activity of cationic antimicrobials via electrostatic binding. In this work, we use synchrotron small-angle X-ray scattering to investigate the interaction between tobramycin, an aminoglycoside antibiotic commonly administered to CF patients via inhalation, with DNA, which is found in high concentrations in the CF airway. We find that interactions between DNA and tobramycin are significantly modified by the presence of mixtures of amphiphilic molecules. We measure a hierarchy of self-assembled structures formed between tobramycin, DNA, and the amphiphile mixtures and show how interactions between these components can be controlled. Results indicate that mixtures of cationic and negative curvature amphiphiles optimized for DNA binding via charge matching and curvature matching can competitively displace bound tobramycin from DNA and thereby drastically suppress tobramycin−DNA binding and resultant antimicrobial inactivation. Growth inhibition assays confirm the increased activity of tobramycin in the presence of DNA with the addition of the amphiphiles. These results suggest that optimized cationic amphiphile solutions have the potential to enhance antimicrobial function in highly infected environments that contain increased concentrations of anionic inflammatory polymers.

1. Introduction

The aim for deterministic control of the interactions between charged macromolecules in aqueous media has motivated widespread experimental and theoretical work. Although it has been well established that like-charged macromolecules can aggregate under the influence of oppositely charged condensing agents, the specific conditions for the stability of such aggregates can only be determined empirically.[1−10] The problem becomes more complex when the condensing agents themselves are spatially extended (such as charged membranes, peptides, globular proteins, or synthetic macromolecules). These condensing agents have their own surface charge distributions, associated counterions, and excluded volumes. Since the major driving force for the attraction between anionic and cationic macromolecules in water is entropy gain from counterion release,[5,11] there is a strong interplay between electrostatic and osmotic effects, the consideration of which is especially important for understanding the interaction between different charged objects of different shapes in salt solutions. This is illustrated by recent work, which shows that electrostatic complexes formed between polyelectrolyte rods (e.g., DNA, filamentous actin (F-actin)) and other oppositely charged macromolecules (e.g., lipids, globular proteins, dendrimers) can adopt a broad range of self-assembled structures.[8−10,12−16]

The structure and stability of these types of electrostatic complexes have important consequences for diseases such as

[†] Department of Materials Science and Engineering.
[‡] Department of Animal Biology.
[§] Department of Physics.
[∥] Department of Bioengineering.
[⊥] Previously published under Kirstin R. Purdy.
[▽] Current address: W. M. Keck Science Center, The Claremont Colleges, Claremont, CA 91711.

(1) Grosberg, A. Y.; Nguyen, T. T.; Shklovskii, B. I. *Rev. Mod. Phys.* **2002**, *74*, 329–345.
(2) Levin, Y. *Rep. Prog. Phys.* **2002**, *65*, 1577–1632.
(3) Bloomfield, V. A. *Curr. Opin. Struct. Biol.* **1996**, *6*, 334–341.
(4) Gelbart, W. M.; Bruinsma, R. F.; Pincus, P. A.; Parsegian, V. A. *Phys. Today* **2000**, *53*, 38–44.
(5) Wong, G. C. L. *Curr. Opin. Colloid Interface Sci.* **2006**, *11*, 310–315.
(6) Olvera de la Cruz, M.; Belloni, L.; Delsanti, M.; Dalbiez, J. P.; Spalla, O.; Drifford, M. *J. Chem. Phys.* **1995**, *103*, 5781–5791.
(7) Angelini, T. E.; Liang, H.; Wriggers, W.; Wong, G. C. L. *Proc. Natl. Acad. Sci. U.S.A.* **2003**, *100*, 8634–8637.
(8) Sanders, L. K.; Guáqueta, C.; Angelini, T. E.; Lee, J-W.; Slimmer, S. C.; Luijten, E.; Wong, G. C. L. *Phys. Rev. Lett.* **2005**, *95*, 108302.
(9) Guáqueta, C.; Sanders, L. K.; Wong, G. C. L.; Luijten, E. *Biophys. J.* **2006**, *90*, 4630–4638.
(10) Sanders, L. K.; Xian, W.; Guáqueta, C.; Strohman, M. J.; Vrasich, C. R.; Luijten, E.; Wong, G. C. L. *Proc. Natl. Acad. Sci. U.S.A.* **2007**, *104*, 15994–15999.
(11) Nelson, P. *Biological Physics: Energy, Information, Life*; W. H. Freeman and Co.: New York, 2004.
(12) Rädler, J. O.; Koltover, I.; Salditt, T.; Safinya, C. R. *Science* **1997**, *275*, 810–813.
(13) Koltover, I.; Salditt, T.; Rädler, J. O.; Safinya, C. R. *Science* **1998**, *281*, 78–81.
(14) Wong, G. C. L.; Tang, J. X.; Lin, A.; Li, Y.; Janmey, P. A.; Safinya, C. R. *Science* **2000**, *288*, 2035–2039.
(15) Evans, H. M.; Ahmad, A.; Ewert, K.; Pfohl, T.; Martin-Herranz, A.; Bruinsma, R. F.; Safinya, C. R. *Phys. Rev. Lett.* **2003**, *91*, 075501.
(16) Raviv, U.; Needleman, D. J.; Li, Y.; Miller, H. P.; Wilson, L.; Safinya, C. R. *Proc. Natl. Acad. Sci. U.S.A.* **2005**, *102*, 11167–11172.

 10.1021/ja803925n CCC: $40.75

cystic fibrosis (CF). Although CF patients do not appear to have an immune deficiency, defects in the cystic fibrosis transmembrane conductance regulator (CFTR), the cyclic AMP-regulated Cl^- ion channel responsible for CF,[17] result in an increased susceptibility to airway infections. Persistent bacterial infections and the accumulation of viscous infected mucus in the airway are the main cause of mortality in CF.[18,19] Additionally, antimicrobial activity in the airway surface liquid (ASL) is found to be significantly reduced.[20,21] This has been attributed to changes in the ionic strength of the ASL,[22] as well as direct electrostatic interactions between endogenous cationic antimicrobials and anionic polyelectrolytes in the airway.[23−25] The inflammatory response to infections leads to the deposition of high concentrations of anionic polyelectrolytes in the airways. These polyelectrolytes include extracellular filaments produced by colonizing bacteria,[26,27] F-actin,[28] DNA[29−34] released from lysed inflammatory cells, and DNA from lysed bacteria. The concentration of DNA in CF sputum can reach as high as 20 mg/mL, comprising 4−10% of the dry weight of CF sputum.[29−31,34] Likewise, the concentration of F-actin is reported to be 0.1−5 mg/mL in CF sputum.[28] Most of the antimicrobials responsible for airway defense are cationic, such as lysozyme, lactoferrin, β-defensin, and LL37. Recent work has shown the extent to which cationic antimicrobial peptides and inflammatory mediators, which are also present in sputum, are inactivated by the anionic polyelectrolytes. These results demonstrate that F-actin and DNA sequester antimicrobial peptides,[23,25] as well as cytokines[35] in CF sputum. Furthermore, condensed aggregates of DNA and F-actin are a common feature of CF sputum.[19] It is believed that cationic antibacterial peptides and proteins constitute a portion of the ligands holding these anionic polyelectrolytes together,[36] hence the availability of such proteins and their resultant antimicrobial activity are significantly diminished. Furthermore, recent X-ray microscopy studies of CF sputum have revealed the presence of ordered, self-assembled aggregates consistent with actin−lysozyme complexation.[10]

This problem of antimicrobial inactivation by anionic polyelectrolytes strongly affects tobramycin, a potent cationic aminoglycoside antibiotic used to treat airway infections caused by *Pseudomonas aeruginosa*, one of the most common opportunistic pathogens in late-stage CF patients.[37] Tobramycin is typically administered parenterally; however, the high doses necessary to surmount poor absorption and long-term exposure can result in toxicity.[38] In order to circumvent the high serum dosages, inhaled tobramycin is routinely used for direct delivery to the lung with varying degrees of success. It has been observed in vitro that the anionic polyelectrolytes present in CF sputum bind to and drastically reduce the activity of cationic antibiotics such as tobramycin.[23,32,39−41] Whereas, previous work has suggested that F-actin is primarily responsible for binding to typical endogenous antimicrobials such as lysozyme, as a consequence of their compatible surface charge densities,[10] it has been shown that high charge density polyelectrolytes such as DNA contribute more to the sequestration of small cationic molecules such as tobramycin.[41,42] Since this binding is primarily an electrostatic effect, it cannot be significantly suppressed via treatment with recombinant human DNase (Pulmozyme, Genentech), which shortens DNA but does not alter its charge density.[44] Due to this sequestration of tobramycin, its biological accessibility can be as low as 1/20th of the available dose.[39] Consequently, there is a significant need for mitigation of this tobramycin inactivation problem.

In this paper, we develop a technique for improving tobramycin activity in the presence of DNA by developing an unbinding agent with a shape and charge density that is optimized to bind to airway polyelectrolytes more readily than does tobramycin. To do this, we first show, using high-resolution synchrotron X-ray diffraction and confocal microscopy, that DNA forms columnar close-packed hexagonal DNA complexes in the presence of tobramycin (cationic charge of +3 to +5, depending on pH), consistent with previous observed condensation behavior of DNA in the presence of multivalent ions.[42,43,45] We then show that it is possible to modify the binding affinity between tobramycin and DNA by adding a solution of cationic amphiphiles that we can optimize by matching the charge density and curvature of the interface between the two binding surfaces. By charge-matching and curvature-matching the cationic amphiphiles to enhance their binding to DNA, these agents competitively displace tobramycin from DNA complexes and form self-assembled lamellar and inverted hexagonal complexes with the DNA,[12−16] which are similar to those used in synthetic

(17) Riordan, J. R.; Rommens, J. M.; Kerem, B.; Alon, N.; Rozmahel, R.; Grzelczak, Z.; Zielenski, J.; Lok, S.; Plavsic, N.; Chou, J.-L.; Drumm, M. L.; Iannuzzi, M. C.; Collins, F. S.; Lap-Chee, T. *Science* **1989**, *245*, 1066–1073.
(18) Welsh, M. J.; Smith, A. E. *Sci. Am.* **1995**, *273*, 52–59.
(19) Sheils, C. A.; Kas, J.; Travassos, A. P. G.; Janmey, P. A.; Wohl, M. E.; Stossel, T. P. *Am. J. Pathol.* **1996**, *148*, 919–927.
(20) Smith, J. J.; Travis, S. M.; Greenberg, E. P.; Welsh, M. J. *Cell* **1996**, *85*, 229–236.
(21) Travis, S. M.; Conway, B. D.; Zabner, J.; Smith, J. J.; Anderson, N. N.; Singh, P. K.; Greenberg, E. P.; Welsh, M. J. *Am. J. Respir. Cell Mol. Biol.* **1999**, *20*, 872–879.
(22) Bals, R.; Weiner, D. J.; Meegalla, R. L.; Accurso, F.; Wilson, J. M. *Am. J. Respir. Cell Mol. Biol.* **2001**, *25*, 21–25.
(23) Weiner, D. J.; Bucki, R.; Janmey, P. A. *Am. J. Respir. Cell Mol. Bio.* **2003**, *28*, 738–745.
(24) Tang, J. X.; Wen, Q.; Bennett, A.; Kim, B.; Sheils, C. A.; Bucki, R.; Janmey, P. A. *Am. J. Physiol.* **2005**, *289*, L599–L605.
(25) Bucki, R.; Byfield, F. J.; Janmey, P. A. *Eur. Respir. J.* **2007**, *29*, 624–632.
(26) Lewis, R. W. *Tex. Rep. Biol. Med.* **1978**, *36*, 33–38.
(27) Lam, J. J.; Chan, R.; Lam, K.; Costerton, J. W. *Infect. Immun.* **1980**, *28*, 546–556.
(28) Vasconcellos, C. A.; Allen, P. G.; Wohl, M. E.; Drazen, J. M.; Janmey, P. A.; Stossel, T. P. *Science* **1994**, *263*, 969–971.
(29) Chernick, W. S.; Barbero, G. J. *Pediatrics.* **1959**, *24*, 739–745.
(30) Potter, J.; Matthews, L. W.; Spector, J. S. *Am. J. Dis. Child.* **1960**, *100*, 493–495.
(31) Matthews, L. W.; Spector, S.; Lemm, J.; Potter, J. L. *Am. Rev. Respir. Dis.* **1963**, *88*, 199–204.
(32) Potter, J. L.; Matthews, L. W.; Spector, S.; Lemm, J. *Pediatrics* **1965**, *36*, 714–720.
(33) Shak, S.; Capon, D. J.; Hellmiss, R.; Marsters, S. A.; Baker, C. L. *Proc. Natl. Acad. Sci. U.S.A.* **1990**, *87*, 14961–14966.
(34) Brandt, T.; Breitenstein, S.; von der Hardt, H.; Tummler, B. *Thorax* **1995**, *50*, 880–882.
(35) Perks, B.; Shute, J. K. *Am. J. Respir. Crit. Care Med.* **2000**, *162*, 1767–1772.
(36) Travis, S. M.; Singh, P. K.; Welsh, M. J. *Curr. Opin. Immunol.* **2001**, *13*, 89–95.
(37) Gibson, R. L.; Burns, J. L.; Ramsey, B. W. *Am. J. Respir. Crit. Care Med.* **2003**, *168*, 918–951.
(38) Cheer, S. M.; Waugh, J.; Noble, S. *Drugs* **2003**, *63*, 2501–2520.
(39) Mendelman, P. M.; Smith, A. L.; Levy, J.; Weber, A.; Ramsey, B. W.; Davis, R. L. *Am. Rev. Respir. Dis.* **1985**, *132*, 761–765.
(40) Hunt, B. E.; Weber, A.; Berger, A.; Ramsey, B.; Smith, A. L. *Antimicrob. Agents Chemother.* **1995**, *39*, 34–39.
(41) Ramphal, M. F. R.; Lhermitte, M.; Filliat, M.; Roussel, P. *J. Anitmicrob. Chemother.* **1998**, *33*, 483–490.
(42) Zribi, O. V.; Kyung, H.; Golestanian, R.; Liverpool, T. B.; Wong, G. C. L. *Phys. Rev. E* **2006**, *73*, 0131911.
(43) Conwell, C. C.; Vilfan, I. D.; Hud, N. V. *Proc. Natl. Acad. Sci. U.S.A.* **2003**, *100*, 9296–9301.
(44) Suri, R. *Biodrugs* **2005**, *19*, 135–144.
(45) Raspaud, E.; Durand, D.; Livolant, F. *Biophys. J.* **2005**, *88*, 392–403.

gene delivery protocols. Using growth inhibition assays, we show that activity of tobramycin against *P. aeruginosa* (PA01) in the presence of DNA is significantly enhanced when cationic amphiphiles are added to displace the tobramycin from the DNA. The in vitro results presented here suggest that cationic amphiphile mixtures can coat the negatively charged DNA found in the ASL of CF patients, leading to the release of the aminoglycoside antibiotics and the increase of their antibacterial activity.

2. Experimental Section

2.1. DNA Preparation. Polydisperse dehydrated calf thymus DNA (USB Corp. Cleveland, OH) is resuspended in Tris−EDTA buffer (pH 8; Ambion Inc. Austin, TX) followed by ethanol precipitation using standard techniques.[46] Purified DNA is then resuspended in either ultrapure water (18.2 MΩ; Millipore, Billerica, MA) or a buffer composed of 5 mM Tris, 5 mM PIPES (piperazine-1,4-bis(2-ethanesulfonic acid)) and 100 mM KCl adjusted to pH 7 or 8. A range of pH's are employed to span physiological conditions in the ASL of CF patients, as previous studies have shown that the pH of airways varies from about 6.5−7.5 for both normal and CF airways.[47]

2.2. Lipid Preparation. The cationic amphiphiles used are lipid suspensions prepared using a mixture of DOTAP (1,2-dioleoyl-3-trimethylammonium-propane), and DOPE (1,2-dioleoyl-*sn*-glycero-3-phosphoethanolamine) (Avanti Polar Lipids, Alabaster AL). Lipids are prepared by dissolving in chloroform, and then mixing at the appropriate mass ratio. DOTAP and DOPE are prepared at ratios of $\Phi_{DOTAP} = 100$, $\Phi_{DOTAP}/\Phi_{DOPE} = 70{:}30$, 30:70, and 25:75, where $\Phi_{DOPE} = [DOPE]/[DOPE + DOTAP]$ and $\Phi_{DOTAP} = [DOTAP]/[DOPE + DOTAP]$ are the mass fractions of the lipids. Suspensions are then dried under nitrogen and desiccated under vacuum overnight. Following desiccation, the lipids are then dissolved into the experimental buffer and incubated at 37 °C for a minimum of 12 h. The aqueous solution is then sonicated to clarity to form unilamellar lipid vesicles, and extruded through 0.2 μm nucleopore membranes (Whatman, Inc., Florham Park, NJ). Freshly prepared liposome solutions are stored at 4 °C and used within 1 week.

2.3. Preparation of Tobraymycin, DNA, Lipid Complexes. Tobramycin, DNA, lipid (TDL) complexes are prepared in ultrapure water or buffer solution (pH 7 or 8). Samples are prepared by first mixing tobramycin (MW = 467.52 g/mol; Sigma Aldrich, St. Louis, MO) with the cationic lipid suspension, as both are positively charged. Resuspended DNA is then added to the mixture to a final fixed concentration of 2−3 mg/mL. Concentrations of DNA, lipids, and tobramycin were determined such that the ratio of positive to negative charges is known. At both pH 7 and 8, the charge of DOTAP was assumed to be +1 e/DOTAP molecule and the charge of the DNA is taken to be −2 e/base pair. The ratio of DOTAP charge to DNA charge is abbreviated as *L*/*D* and was kept fixed while the concentration tobramycin was varied. The ratio of tobramycin charge to DNA charge is abbreviated as *T*/*D*. The charge of the tobramycin was determined to vary as a function of pH as discussed below. After mixing DNA with lipids and/or tobramycin, the solution, including any complexes which formed, are transferred to a 1.5 mm quartz capillary (Charles Supper Co., MA).

2.4. X-ray Diffraction. Quartz capillaries containing TDL mixtures are flame-sealed and centrifuged to force the TDL complexes to pellet. Small-angle X-ray scattering (SAXS) experiments are performed on pelleted samples both at 9 KeV at beamline 4-2 of the Stanford Synchrotron Radiation Laboratory (SSRL; Menlo Park, CA) and at 12 KeV the BESSRC-CAT (beam line 12-ID) at the Advanced Photon Source (APS; Argonne IL). The scattered radiation is collected using an MAR Research (Evanston, IL) charge-coupled device camera (pixel size = 79 × 79 μm^2) at both beamlines. The sample-to-detector distances are set such that the detecting range is $0.5 < q < 4$ nm^{-1}, where $q = (4\pi \sin\theta)/\lambda$, λ is the wavelength of the incident beam, and 2θ is the scattering angle. The 2D SAXS data from both set-ups have been checked for mutual consistency.

2.5. Confocal Microscopy. Microscopy samples are prepared as follows. DNA is diluted to 0.03 mg/mL and incubated with YOYO-1 (Invitrogen, Carlsbad, CA) at a ratio of 1 dye molecule: 20 base pair for 1 h. 25:75 DOTAP/DOPE was prepared as above with the addition of 1% rhodamine-PE (1,2-dioleoyl-*sn*-glycero-3-phosphoethanolamine-*N*-(lissamine rhodamine B sulfonyl)(ammonium salt)) (excitation 550 nm, emission 590 nm; Avanti Polar Lipids, Alabaster AL) and then added to the DNA solution such that $L/D = 0.5$ or 1. For samples containing both tobramycin and cationic lipids, anionic DNA was added to the solution last. Confocal fluorescence microscopy images were taken on a Leica SP2 microscope in sequential line scan mode at the Beckman Institute (Urbana, IL).

2.6. Antimicrobial Activity Assay. Microbroth dilution assays are performed to assess the extent to which the addition of lipids inhibits tobramycin sequestration. All assays follow a modified version of the National Committee for Clinical Laboratory Standards[48] microdilution protocol. Tobramycin stock solutions are prepared at 10 mg/mL, while DNA solutions are prepared at 8 mg/mL. Lipid stock solutions are prepared at 20 mg/mL for specific lipid ratios ($\Phi_{DOTAP} = 100$, $\Phi_{DOTAP}/\Phi_{DOPE} = 70{:}30$, 30:70, and 25:75). As with the X-ray TDL samples, tobramycin is well mixed with the lipid solution before the DNA solution is added. In order to ensure that all samples are prepared in the same manner, control solutions, tobramycin-only solutions, and tobramycin assay solutions in the presence of DNA or DNA/lipid solutions, are prepared in Millipore (Billerica, MA) Amicon Ultra-4 centrifugal filtration units, which have a nominal molecular weight limit (NMWL) of 10 kDa. Approximately 1.5 mL of tobramycin only, tobramycin−DNA, tobramycin−DNA−lipid, and control solutions (buffer only, tobramycin−lipid, lipid only, DNA only) are prepared at 10× concentrations, such that the tobramycin concentration is ∼0.29 mg/mL. Once the solutions are prepared in the filter units, they are allowed to equilibrate at room temperature for ∼2 h to allow for complexation of the constituents. The solutions are then centrifuged at 5000*g* in a Beckman Instruments (Fullerton, CA) Avanti J-25 centrifuge for 2−4 h at 4 °C to completely separate unbound tobramycin from complexes. The resulting supernatant from the tobramycin assay solutions are then diluted 10× by adding cation adjusted Mueller−Hinton broth (MH; pH 7.4), so that the final concentration of the "tobramycin-only" assay stock solution is ∼0.029 mg/mL. The final assay solutions (104 μL) are then added to a 96-well plate and a 2-fold serial dilution is performed, such that the final concentrations of the "tobramycin only" assay solutions ranged from 25 to 0.1 μg/mL.

P. aeruginosa (PAO1) from a freshly streaked agar plate were grown overnight in MH broth. From the overnight culture, a 100× dilution was incubated at 37 °C for ∼2 h or until the culture density equaled a 0.5 McFarland turbidity standard, which represents ∼10^8 CFU/mL.[48] The 2 h growth was then diluted ∼125× so that the final PAO1 concentration in the 96-well plate was ∼10^5 CFU/mL. A 16 μL aliquot of the PAO1 solution is added to each experimental well of the 96-well plate by using a multipipette. Positive control wells contained PAO1 only while the negative control wells contained MH only. After the PAO1 addition, the 96-well plates are mixed using a microplate shaker for ∼30 s, sealed with parafilm and placed in a 35 °C incubator for 24 h. After 22 h, the plates are

(46) Sambrook, J.; Russell, D. W. *Molecular Cloning*, 3rd ed.; Cold Spring Harbor Laboratory Press: Cold Spring Harbor, NY, 2001; Vol. 3.
(47) McShane, D.; Davies, J. C.; Davies, M. G.; Bush, A.; Geddes, D. M.; Alton, E. W. F. W. *Eur. Respir. J.* **2003**, *21*, 37–42.
(48) National Committee for Clinical Laboratory Standards. *Methods for Dilution Antimicrobial Susceptibility Tests for Bacteria That Grow Aerobically—Fifth Edition: Approved Standard M7-A5*; NCCLS, Wayne, PA, 2000.

mixed for ~30 s on a microplate shaker before returning to the incubator for the remaining 2 h, after which the optical density (OD_{600}) is measured. The minimum inhibitory concentration (MIC_{90}) is determined to be the lowest concentration of antimicrobial agent that prevents visible growth of an overnight culture. Each 96-well plate contained duplicate trials and a minimum of six plates or 12 data sets were collected.

3. Results and Discussion

Much recent progress has been made in our understanding of electrostatic complexes,[5] such as those between cationic tobramycin and anionic DNA. Entropy gain from counterion release is the major driving force in the formation of anionic−cationic complexes in aqueous media. The spatial distribution of counterions around a given macroion, however, is determined by its shape and charge density. In this report we use cationic amphiphiles as tobramycin unbinding and DNA sequestration agents given that their shape and charge density can be independently optimized in a facile and well-controlled manner. Specifically, we use DOPE, a neutral lipid with negative curvature, which is naturally found in eukaryotic cell membranes and is one of the principal neutral lipids in use in gene therapy applications,[49] and DOTAP, a cationic lipid (charge of +1) with approximately zero intrinsic curvature. It has been previously shown that in a mixture of DNA and these lipids, if $\Phi_{DOPE} < 0.41$, a lamellar complex of lipid−DNA stacks, referred to as the L_α^C phase, will form, where the DNA is ordered in a 1D lattice with a well defined spacing d_{DNA}[13]. Increasing the negative spontaneous curvature of the lipid monolayer ($0.7 < \Phi_{DOPE} < 0.85$) induces instead a columnar inverted-hexagonal H_{II}^C phase, where the lipid monolayers wrap around individual DNA filaments, which are arranged in a hexagonal lattice.[13] Coexistence between lamellar and inverted hexagonal phases arises at intermediate values of Φ_{DOPE}. Furthermore, the addition of divalent and trivalent ions to the lamellar cationic lipid−DNA (CL−DNA) complexes has been shown to induce 2D DNA condensation within lamellar complexes.[50] Below we present results showing the different observed phases for DNA and for CL−DNA complexes in the presence of the multivalent cation tobramycin.

3.1. Tobramycin−DNA Complex Formation. DNA condenses into 'bundled' close-packed hexagonal aggregates in the presence of multivalent ions when the DNA and ions are at an isoelectric ratio ($T/D = 1$).[51] Tobramycin is a multivalent ion with a charge between +3 and +5 at physiological pH. We use SAXS to quantitatively examine the effect of pH on the condensation of DNA by tobramycin, in the absence of lipids, and to confirm the charge of tobramycin at different pH. The circularly averaged diffraction spectra for the tobramycin−DNA complexes formed as a function of tobramycin concentration are summarized in Figure 1. In water, 1.85 mM tobramycin condenses 4.5 mM DNA, as indicated by the appearance of a diffraction peak at 2.5 nm^{-1} (Figure 1a); in pH 7 buffer, only 1.7 mM is needed (Figure 1b); and in pH 8 buffer, 3.0 mM is required (Figure 1c). The different amounts of tobramycin needed to condense DNA imply that under different buffer conditions, tobramycin has a different charge. If we assume that the concentrations of DNA and tobramycin in solution are

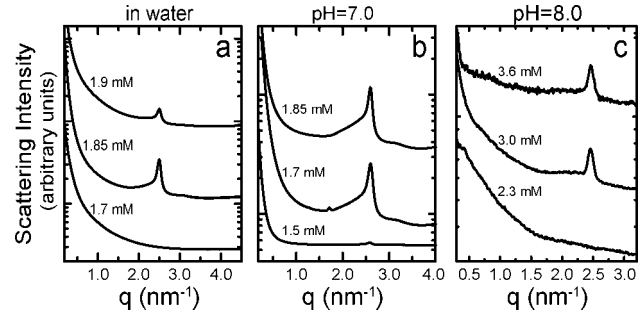

Figure 1. Tobramycin induces the formation of a close-packed hexagonal DNA bundle structure. Circularly averaged diffraction spectra from mixtures of tobramycin with DNA (3 mg/mL) are plotted as a function of increasing tobramycin concentration in (a) water, (b) buffer at pH 7, and (c) buffer at pH 8. Suspensions are buffered at their respective pH in 5 mM Tris, 5 mM PIPES, and 100 mM KCl. The appearance of a peak at ~2.5 nm^{-1} indicates the onset of DNA condensation by tobramycin. The onset of the close-packed bundle peak was used to define $T/D = 1$.

isoelectric ($T/D = 1$) when bundling of the DNA begins,[51] we find that the charge of tobramycin is ~ +5 in H_2O, +5 at pH 7, and +3 at pH 8. These results agree well with previously published values for the charge of tobramycin[52] and show that our results are self-consistent. Tobramycin is electrostatically bound in these tobramycin−DNA complexes, and therefore, would be unavailable for interaction with bacteria in DNA-containing CF airway surface liquid. Below this isoelectric charge ratio (and in the presence of excess DNA), however, tobramycin sequestration still occurs due to electrostatic attraction.[40] Electrostatic interactions favor the binding of tobramycin to DNA at any concentration, limited only by diffusion. In this work, we use cationic lipids to sequester DNA into complexes, which should correspondingly limit the amount of electrostatically driven tobramycin binding.

3.2. Microscopy of Tobramycin−DNA−Cationic Lipid Complexes. Using confocal fluorescence microscopy, we investigated the self-assembly of mixtures of tobramycin, DNA, and cationic lipid solutions. Representative images of colocalization studies are shown in Figure 2. In all images, the tobramycin to DNA charge ratio is equal to $T/D = 1$, while the lipid-to-DNA charge ratio varies from $L/D = 0.5$ (Figure 2a,b) to 1.0 (Figure 2c,d). When cationic lipids are insufficient to neutralize tobramycin charge, only a fraction of the DNA (Figure 2a) is co-localized with the lipids (Figure 2b). The remaining DNA is condensed by tobramycin alone. When the lipid concentration is increased to $L/D = 1$, the DNA colocalizes consistently with the lipids (Figure 2c,d). These results suggest that cationic amphiphiles are attracted to the DNA via electrostatic interactions when their charge densities are favorably matched.[53] We employed SAXS to obtain a more detailed structural picture of this self-assembly process between DNA, tobramycin, and cationic lipids.

3.3. Formation of Lamellar Tobramycin−DNA−Cationic Lipid Complexes. We performed a series of SAXS experiments for which we prepared TDL suspensions at physiological salt and pH conditions. Figure 3 shows the circularly averaged SAXS spectra for electrostatic complexes formed between tobramycin, DNA and a 70:30 DOTAP/DOPE lipid mixture at pH 7. The lipid concentration is set either to be sufficient to neutralize the DNA charge at the isoelectric point ($L/D = 1$) or as overcharged $L/D = 2$ complexes. Lamellar complexes in

(49) Ewert, K.; Slack, N. L.; Ahmad, A.; Evans, H. M.; Lin, A. J.; Samuel, C. E.; Safinya, C. R. *Curr. Med. Chem.* **2004**, *11*, 133–149.
(50) Koltover, I.; Wagner, K.; Safinya, C. R. *Proc. Natl. Acad. Sci. U.S.A.* **2000**, *97*, 14046–14501.
(51) Bloomfield, V. A. *Biopolymers* **1997**, *44*, 269–282.
(52) Szilagyi, L.; Pusztahelyi, Z. S.; Jakab, S.; Kovics, I. *Carbohydr. Res.* **1993**, *247*, 99–109.
(53) Lau, A. W. C.; Pincus, P. *Eur. Phys. J. B* **1999**, *10*, 175–180.

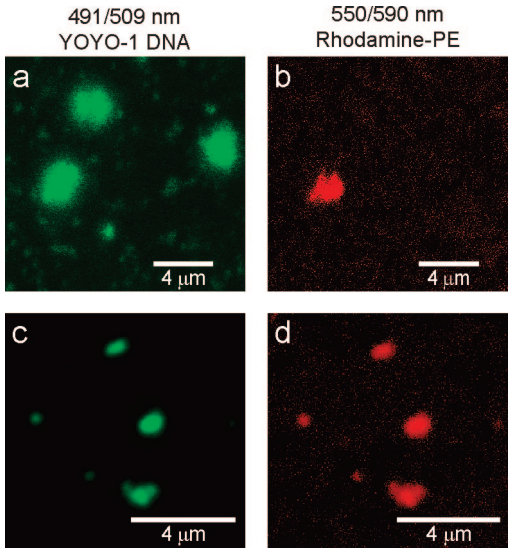

Figure 2. Representative two-channel (false-colored green and red) confocal fluorescence microscopy images of suspensions of DNA and tobramycin ($T/D = 1$) in the presence of suspensions of 25:75 DOTAP/DOPE ($L/D =$ 0.5 for a,b; $L/D = 1$ for c,d) are shown. DNA is labeled with YOYO-1, which is excited by a 488 nm laser, while cationic lipid solution is doped with rhodamine−PE, which is excited by a 550 nm laser. For $L/D = 0.5$ complexes, DNA aggregates (a,b) are only partially co-localized with lipids (b), but when $L/D = 1$ the DNA is fully co-localized with lipids (c,d).

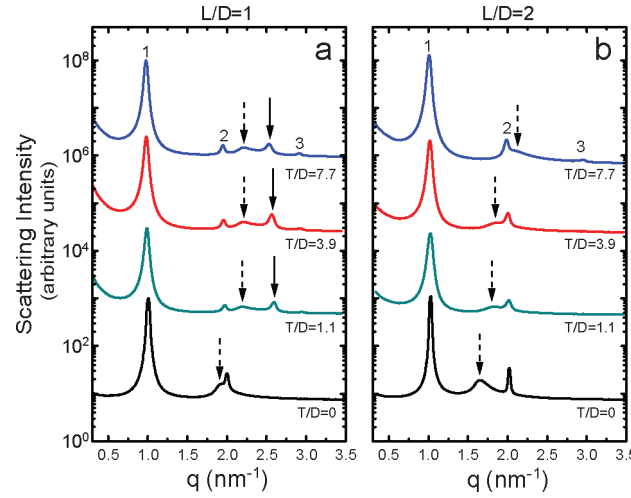

Figure 3. Relative stability of the close-packed tobramycin−DNA bundle phase and the lamellar tobramycin−DNA−cationic lipid phase depends on the cationic lipid to DNA ratio. Circularly averaged diffraction spectra from L_α^C forming TDL complexes containing 3 mg/mL DNA is plotted as a function of increasing T/D for (a) 70:30 DOTAP/DOPE at $L/D = 1$ and (b) 70:30 DOTAP/DOPE at $L/D = 2$. Tobramycin charge is +5 at pH 7. Indexed peaks correspond to the lamellar phase of the CL−DNA complex. Dashed arrows show the 2D (within the lipid bilayers) inter-DNA spacing and solid arrows indicate close-packed tobramycin−DNA bundles.

which DNA is sandwiched between lipid bilayers in a 2D smectic phase[12] are formed in both cases. However, the relative stability of these lamellar complexes with respect to the close-packed hexagonally ordered tobramycin−DNA aggregates in these two cases is qualitatively different and depends on the overcharging (L/D ratio).

For the isoelectric case of $L/D = 1$, where we have approximate charge density matching between the cationic amphiphile and DNA, we find that the 70:30 DOTAP/DOPE lipid mixtures form lamellar complexes with DNA in the presence of tobramycin. At pH 7 (Figure 3a,b) the lamellar peak positions occur at $q_1 = 0.99$, $q_2 = 1.99$, and $q_3 = 2.92$ nm^{-1}. Lamellar peak positions are similar for other buffer conditions (data not shown): $q_1 = 1.03$, $q_2 = 2.04$, and $q_3 = 3.02$ nm^{-1} for unbuffered solution, and $q_1 = 0.97$, $q_2 = 1.99$, and $q_3 =$ 2.91 nm^{-1} for pH 8. As the added tobramycin concentration increases, the DNA correlation peak, indicated by the dashed arrow, shifts toward higher q, showing that the inter-DNA distance within the lamellar structure, d_{DNA}, decreases until the DNA become nearly close packed at d_{DNA}= 2.85 nm (Figure 4). The shift in q-position of the 2D smectic peak toward higher q with increased concentrations of tobramycin is consistent with previous measurements of the 2D DNA condensation by divalent and trivalent ions in the presence of cationic lipids[50] and has been shown to be due to the infiltration of additional multivalent ions within the complex.[60,61] This increased multivalent ion concentration leads to decreased electrostatic repulsion between DNA chains. As the tobramycin concentration is increased, the inter-DNA spacing of the 2D smectic phase decreases continuously, until a critical concentration, at which the inter-DNA spacing takes a discontinuous jump to the close-packed inter-DNA separation of the 2D condensed raft phase. This abrupt transition is likely first order, and is the result of multivalent cation mediated 'like-charge' attraction between DNA.[50] The inter-DNA distance in the 2D condensed raft phase is slightly larger than the hydrated diameter of DNA (~2.5 nm) suggesting that tobramycin is tightly bound between adjacent DNA, condensing the DNA into a close-packed cross-linked structure between the lipid sheets. In Figure 3a, we also show that, for the isoelectric case of $L/D = 1$, when $T/D > 1$, tobramycin forms close-packed tobramycin−DNA bundles at the expense of the 2D condensed raft phase of the CL−DNA complexes, as indicated by the peaks labeled with the solid arrow.

The behavior of the overcharged lamellar complexes ($L/D > 1$) is drastically different (Figure 3b). No formation of tobramycin−DNA complexes is observed as T/D is increased, even when the total tobramycin charge exceeds that of the lipids by a factor of 2 ($T/L > 2$). This inhibition of the close-packed tobramycin−DNA bundle formation implies that less tobramycin is sequestered by DNA and that higher levels of antimicrobial activity may be restored when additional cationic lipids are added ($L/D > 1$). As tobramycin is added, however, the internal structure of the lamellar complexes is still altered in this overcharged lamellar complex (Figure 3b). As with the $L/D = 1$ suspensions, the shifting DNA correlation peak shows that the inter-DNA distance gradually decreases as the DNA is progressively condensed until close-packed within the lamellar complexes. This observed condensation is induced by tobramycin which has still partially infiltrated the complex. These results suggest that lamellar complexes, in which the surface

(54) Harries, D.; May, S.; Gelbart, W. M.; Ben-Shaul, A. *Biophys. J.* **1998**, *75*, 159–173.
(55) Britt, M. R.; Garibaldi, R. A.; Wilfert, J. N.; Smith, C. B. *Antimicrob. Agents Chemother.* **1972**, *2*, 236–241.
(56) Ioannides-Demos, L. L.; Liolios, L.; Wood, P.; Spicer, W. J.; McLean, A. J. *Antimicrob. Agents Chemother.* **1998**, *42*, 1365–1369.
(57) Andrews, J. M. *J. Antimicrob. Chemother.* **2001**, *48*, 5–16.
(58) Jiang, L.; Patel, D. J. *Nat. Struct. Biol.* **1998**, *5*, 769–774.
(59) Vicens, Q.; Westhof, E. *Chem. Biol.* **2002**, *9*, 747–755.
(60) Liang, H.; Angelini, T. E.; Braun, P. B.; Wong, G. C. L. *J. Am. Chem. Soc.* **2003**, *125*, 11786–11787.
(61) Liang, H.; Angelini, T. E.; Braun, P. B.; Wong, G. C. L. *J. Am. Chem. Soc.* **2004**, *126*, 14157–14165.

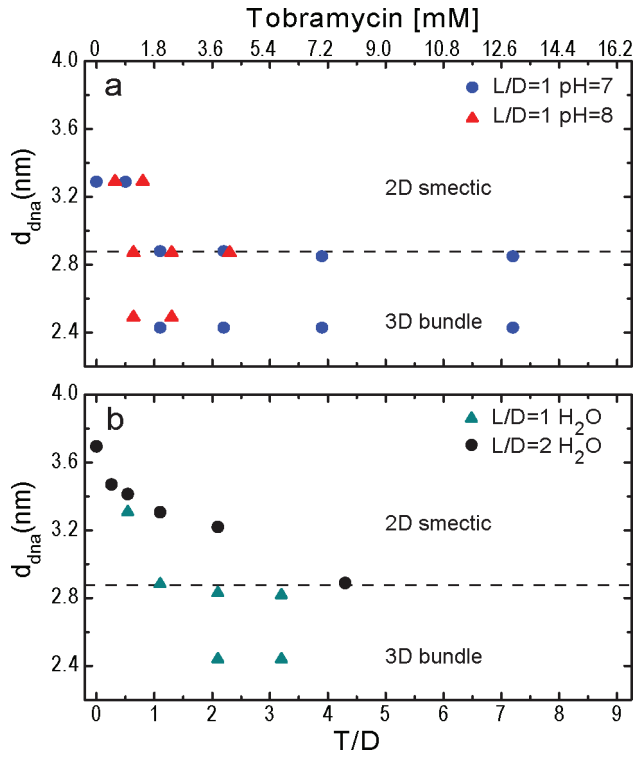

Figure 4. Measured inter-DNA spacing for the close-packed tobramycin−DNA bundle phase and the coexisting lamellar tobramycin−DNA−cationic lipid phase as a function of *T*/*D* ratio under different buffer conditions (a) and *L*/*D* charge ratios (b). The top axis indicates tobramycin concentration for samples prepared with 3 mg/mL DNA at pH 7 ($q_T = +5$). Ratio of cationic to curved lipids was fixed at 70:30 DOTAP/DOPE. Tobramycin, DNA, and cationic lipids are organized into three phases: a 2D smectic phase with DNA intercalated between lipid sheets, a 2D condensed raft phase with DNA essentially close-packed between lipid sheets (dashed line), and a close-packed 3D tobramycin−DNA bundle phase. A comparison of $L/D = 1$ complexes prepared at different pH values (a), shows that with increasing *T*/*D*, DNA within the lamellar CL−DNA complex is first oriented in a 2D smectic phase, then close-packed into a 2D condensed raft phase with $d_{DNA} = 2.85$ nm, and then condensed into tobramycin−DNA bundles with an inter-DNA spacing of 2.45 nm. However, above $T/D = 3$, the bundling is no longer present at pH 8 conditions (a, red triangles). At lipid to DNA charge ratios above $L/D = 1$, the DNA shows only a 2D condensed raft phase (dashed line) at high tobramycin concentrations and formation of tobramycin−DNA bundles is completely inhibited (b, black circles).

charge density of the cationic membrane is approximately matched to that of DNA, do not completely exclude tobramycin from DNA binding, even when extra lipids are added to the solution.

The observed structural trends for this composite system are summarized in Figure 4, which shows the conditions required for different organizations of DNA, tobramycin, and cationic lipids. A 2D smectic phase intercalated between lipid sheets, a 2D condensed raft phase intercalated between lipid sheets, and a close-packed tobramycin−DNA bundle phase with no lipids were determined from measurements of the inter-DNA spacing peaks in the SAXS data. In Figure 4a, we compare the observed phase behavior for solutions at pH 7 and 8, where tobramycin has a charge of +5 and +3, respectively. For $T/D < 3$, samples prepared at both buffer conditions exhibit similar phases for a given tobramycin to DNA charge ratio. From Figure 4a, it is clear that the density of DNA packing depends only on *L*/*D* and *T*/*D* and not on absolute tobramycin concentration. The trend to suppress tobramycin−DNA complexes as *L*/*D* increases from 1 (isoelectric) to 2 (overcharged), as shown in Figure 3 for pH 7 buffered solutions is also confirmed in Figure 4b for TDL suspensions created in ionized water solutions. Since the pH of the ASL is unknown and uncontrollable, we modeled a range of conditions by measuring the TDL complex formation in water as well as in buffered solutions. In Figure 4b, as *L*/*D* increases, less close-packed tobramycin−DNA bundles are formed at the same ratio of *T*/*D*, indicating less tobramycin is bound to the DNA. However, the data also indicates that the CL−DNA complexes also sequester some tobramycin, as evidenced by the decrease in inter-DNA distance, and corresponding increase in DNA density, within the complexes. As the global concentration of tobramycin increases, cationic tobramycin infiltrates the complex, which decreases repulsion between anionic DNA and cross-links the DNA at small separations. Due to the tendency for charge neutralization in systems of DNA and cations,[42,62] the amount of tobramycin bound to DNA should be significantly less in these CL−DNA complexes than in the 3D tobramycin−DNA bundle, due to both the partial charge neutralization of the anionic DNA charge by the cationic lipids, and geometric confinement of the tobramycin to the 2D space between the DNA molecules (limited by the CL−DNA membranes). Thus, by controlling the CL−DNA complex formation, we can maximize electrostatic binding of DNA to the cationic lipids and minimize binding of tobramycin to DNA. In other words, by matching the charge density of the cationic membrane to that of anionic DNA, we are in essence using an electrostatic mechanism to inhibit binding between tobramycin and DNA. It can be seen that this electrostatic mechanism is imperfect, since tobramycin infiltration into the complex is still possible. We also examine a complementary mechanism, based on steric exclusion of tobramycin. Specifically, the intrinsic curvature of the amphiphilic membrane can be tuned to allow wrapping, as well as electrostatic passivation of the DNA.[53,54] One example of such a phase is the inverted hexagonal H_{II}^C phase, which should not have sufficient room near the DNA−lipid interface to sterically allow for significant tobramycin binding. We test this hypothesis in the next section.

3.4. Inverted Hexagonal Tobramycin−DNA−Cationic Lipid Complexes. In order to assess the proposed design principle of using cationic amphiphiles with optimized intrinsic curvature for DNA binding, we studied TDL suspensions containing a mixture of cationic and negative curvature lipids at a ratio that forms an H_{II}^C inverted hexagonal CL−DNA complex in the absence of tobramycin.[13] The inverted hexagonal complexes require a design tradeoff: in order to have the negative intrinsic curvature to wrap the DNA and thereby inhibit tobramycin binding sterically, less cationic lipids with bulky headgroups can be incorporated into the membrane, which will lead to a surface charge density mismatch between the DNA and the charged membrane. The structures formed from TDL mixtures containing a range of different concentrations of 25:75 DOTAP/DOPE were examined. In Figure 5, we show the circularly averaged SAXS spectra for representative TDL complexes formed using 25:75 DOTAP/DOPE lipid mixtures at pH 7. Diffraction peaks corresponding to an inverted hexagonal CL−DNA complex are observed for both isoelectric ($L/D = 1$) and overcharged ($L/D = 2$) lipid−DNA concentrations at all tobramycin concentrations. Furthermore, a tobramycin−DNA bundle peak is observed at $q_{DNA} = 2.60$ nm^{-1}, in coexistence with the inverse hexagonal diffraction peaks, but only for $T/D > 1$. Interestingly, this transition from purely H_{II}^C

(62) Zribi, O.; Kyung, H.; Golestanian, R.; Liverpool, T.; Wong, G. C. L. *Europhys. Lett.* **2005**, *70*, 541–547.

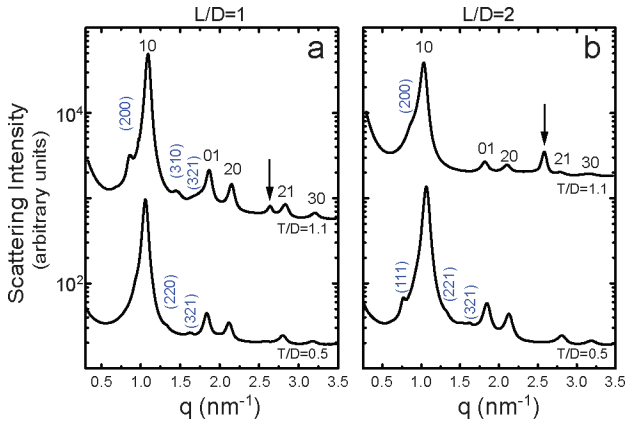

Figure 5. Lipids with optimized intrinsic curvature suppress formation of close-packed tobramycin−DNA bundles, and form inverted hexagonal DNA−lipid complexes with sterically expelled DNA. Circularly averaged diffraction from TDL complexes is shown as a function of increasing tobramycin concentration (represented as the ratio of tobramycin charge to DNA charge T/D assuming $q_T = +5$) for 25:75 DOTAP/DOPE complexed with 2.5 mg/mL DNA at $L/D = 1$ (a) and 2 (b) in pH 7 buffer (5 mM Tris, 5 mM PIPES, 100 mM KCl). Indexed peaks correspond to an H_{II}^C inverse hexagonal phase. Solid arrows at $q \approx 2.60$ nm^{-1} indicate diffraction from close-packed tobramycin−DNA bundles. Horizontal numbers show the indexing of the 2D columnar hexagonal phase. Vertical numbers (blue) correspond to a phase-separated *Pn3m* cubic, presumably rich in DOPE. These extra peaks were observed at all investigated T/D ratios and are not surprising as tobramycin essentially acts as a multivalent salt and excess lipid is often expelled from the lipid−DNA complex when $\Phi_{DOTAP} < 0.5$ and salt concentrations are high (>100 mM for $\Phi_{DOTAP} = 0.3$).[13,50]

to H_{II}^C coexisting with close-packed tobramycin−DNA bundles is insensitive to the L/D ratio, in contrast to the lamellar complexes (Figure 3b vs Figure 5b). At pH 7, the tobramycin concentration independent diffraction peaks occur at $q_{10} = 1.06$, $q_{01} = 1.83$, $q_{20} = 2.12$, $q_{21} = 2.80$, and $q_{30} = 3.18$ nm^{-1} and index to a hexagonal symmetry. Experiments performed with 30:70 DOTAP/DOPE lipid mixtures in ionized water (data not shown) show slightly shifted peaks at $q_{10} = 1.08$, $q_{01} = 1.90$, $q_{20} = 2.18$, $q_{21} = 2.90$, and $q_{30} = 3.30$ nm^{-1} which clearly still index according to a hexagonal symmetry. Both data sets correspond to a 2D columnar inverted hexagonal structure (H_{II}^C), in which DNA is wrapped by lipid monolayers and organized into hexagonal arrays. Within this structure, the center-to-center interaxial DNA spacing $[4\pi/\sqrt{(3q_{10})}]$ is 67.8−69.4 Å in pH 7 buffer and 66.6−67.1 Å in H_2O. The small shift in peak positions between buffered and unbuffered (water) solutions is presumably due to the differences in ionic strength and DNA surface charge in these solutions. These hexagonally indexed peaks appear in the absence of tobramycin ($T/D = 0$), and the spacing of the H_{II}^C phase is clearly independent of tobramycin concentration, as the peaks do not shift with T/D.

It is interesting to note that no tobramycin−DNA complexes are observed for $T/D < 1$. This is relevant to CF treatment as typical tobramycin and DNA concentrations found in the airway surface liquid of CF patients correspond to $T/D \ll 1$.[29−31,34,39,41] Because of the intrinsic curvature of the composite lipid membrane, which wraps around the individual DNA strands, tobramycin access to the DNA is limited by steric effects. Inclusion of tobramycin in the inverted hexagonal complex will necessarily require structural defects and incur a free energy penalty. In principle, this will tend to expel tobramycin and thereby increase its bioavailability.

From the above, it can be seen that the surface charge density matched lamellar system excludes tobramycin electrostatically,

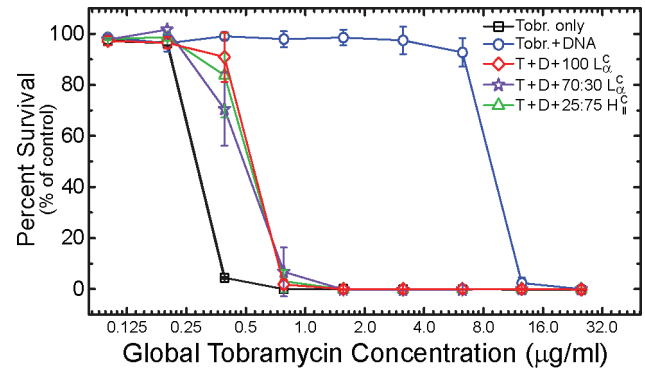

Figure 6. Growth inhibition assay results show that cationic amphiphiles increase the concentration of free tobramycin in the presence of high concentrations of DNA. The percent survival of *P. aeruginosa* in the presence of increasing concentrations of tobramycin is shown for five cases. The results indicate that the tobramycin allowed to interact with DNA at $T/D = 0.5$ (blue circles) shows a significant reduction in killing efficiency as compared to free tobramycin (black squares). When cationic lipids ($L/D = 1$) are present in addition to DNA and tobramycin, a marked recovery of killing is observed (100% DOTAP (red circles); 70:30 DOTAP/DOPE (purple stars); 25:75 DOTAP/DOPE (green triangles)).

while the curvature matched inverted hexagonal system excludes tobramycin sterically. In the following section we compare the ability of lamellar and inverted hexagonal complexes to increase tobramycin efficacy in the presence of DNA using growth inhibition assays.

3.5. Recovery of Tobramycin Antimicrobial Activity from DNA-Rich Solutions with Addition of Cationic Amphiphiles. To independently evaluate the extent to which cationic lipids liberate tobramycin from DNA complexes, we employ microbroth dilution growth inhibition assays, which are commonly used to determine the minimum inhibitory concentrations (MIC_{90}) of antibiotics on various bacterial strains.[48] As shown in Figure 6, free tobramycin (black squares) shows a MIC_{90} of ~0.4 μg/mL, which is within the range of expected values for the MIC_{90} of tobramycin.[55−57] However, when tobramycin is allowed to first bind with DNA ($T/D = 0.5$), the killing efficiency of tobramycin is drastically reduced by a factor of approximately 30× to an increased MIC_{90} of ~12.5 μg/mL (Figure 6, blue circles). This is consistent with the self-assembly behavior measured by X-ray diffraction experiments described above, which indicate that when $T/D > 1$ DNA sequesters tobramycin into close-packed tobramycin−DNA bundles (Figure 2) and furthermore confirms that even when $T/D < 1$ a significant amount of tobramycin is sequestered by DNA in the absence of cationic lipids, even though structural changes are not observed in SAXS.

We compare growth inhibition assay results for three different amphiphilic formulations, two that form lamellar complexes (DOTAP = 100; DOTAP/DOPE = 70:30, $L/D = 1$) and one that forms inverted hexagonal complexes (DOTAP/DOPE = 25:75, $L/D = 1$). We included 100% DOTAP complexes to determine if increasing the charge would enhance the repulsion of tobramycin from the lamellar complexes. It can be seen that each lipid formulation leads to a significant recovery of tobramycin activity. The measured MIC for both the inverted hexagonal phase (green triangles) and the lamellar phases (100% DOTAP, red diamonds; 70:30 DOTAP/DOPE, purple stars) decreases to 0.8 μg/mL, which indicates a 15-fold improvement of tobramycin activity compared to the results in the presence of DNA only. Since the DNA self-assembles with the lipid to form high-molecular-weight complexes, both are unable to pass

through the centrifuge filter and are not available to interact with the bacteria, and therefore not able to contribute a potentially confounding influence. Additionally, all controls (tobramycin−lipid only; lipid only; DNA only) showed no sign of enhanced bacterial killing or of enhancement in bacteria growth (data not shown). The combination of these results indicates that the cationic amphiphiles can indeed displace tobramycin in this assembly process, thereby releasing sequestered tobramycin and increasing its bioavailability (Figure 6). The electrostatic exclusion mechanism of the lamellar phase and the steric exclusion mechanism of the inverted hexagonal phase do not lead to significant differences in bacterial growth inhibition, as they both involve design trade-offs. However, it can be seen that even with imperfect electrostatic exclusion of tobramycin or imperfect steric exclusion of tobramycin, most of the activity of tobramycin can be recovered. That there are two distinct ways to accomplish this is also promising, as this potentially allows for more clinical flexibility.

4. Conclusions

We have shown that we can limit the binding and self-assembly between DNA and tobramycin by adding a solution of cationic lipids to the tobramycin−DNA suspension. We find that DNA interacts preferentially with cationic lipids for a broad range of tobramycin concentrations, as long as the tobramycin concentration is less than that required neutralize the DNA charge ($T/D = 1$). When the tobramycin concentration increases above that required for DNA charge neutralization, close-packed tobramycin−DNA bundles with high concentrations of sequestered tobramycin are observed. A schematic phase diagram with representations of the different observed self-assembled structures is shown in Figure 7. For lipids that form a lamellar phase with the DNA (Figure 7a), tobramycin is consistently incorporated into the cationic lipid−DNA complex and thereby sequestered. By increasing the ratio of cationic lipid to tobramycin charge, it is possible to partially suppress the formation of close-packed DNA bundles, which sequester high concentrations of tobramycin. When we use a lipid formulation that includes negative curvature lipids in addition to cationic lipids (Figure 7b), the DNA−lipid complex forms an inverse hexagonal phase, which, by coating the anionic DNA, suppresses electrostatic binding between DNA and tobramcyin, as well as sterically suppresses tobramycin intercalation within the complexes at concentrations similar to those in typical therapeutic doses, hence minimizing tobramycin sequestration. We have identified two distinct mechanisms for inhibition of DNA tobramycin binding: one based on electrostatic interactions and one based on steric interactions. From growth inhibition assay results, we confirmed that tobramycin activity in the presence of DNA is significantly enhanced by the addition of such cationic lipid formulations, as indicated by a >15× MIC improvement. Having two different mechanisms for tobramycin activation potentially allows for more clinical flexibility in choosing different amphiphilic mixtures to improve tobramycin efficacy in vivo.

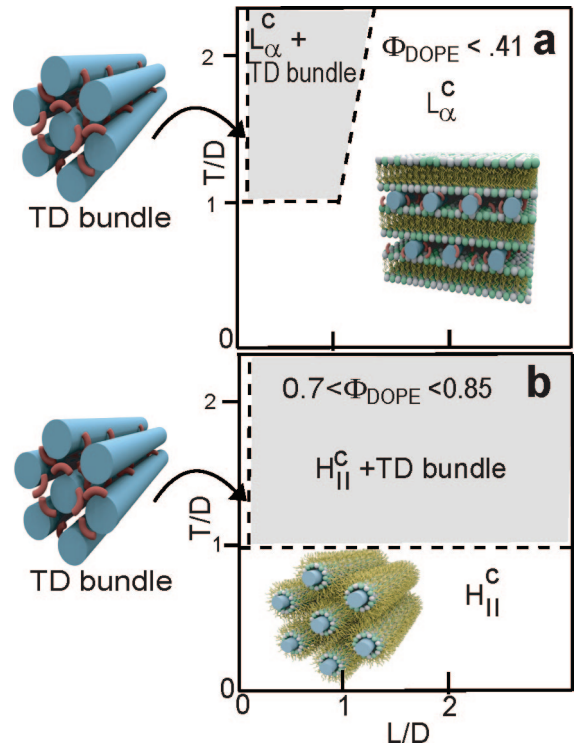

Figure 7. Schematic phase diagrams showing different self-assembled TDL structures observed as a function of tobramycin-to-DNA charge ratio (*T*/*D*) and lipid-to-DNA charge ratio (*L*/*D*) for the lamellar (a) and inverse hexagonal phase forming CL−DNA complexes (b), assuming a fixed DNA concentration. Dashed lines show approximate boundaries between single phase regions and the shaded coexistence region where both tobramycin−DNA close-packed bundles (TD bundle) and the CL−DNA complexes are observed. Tobramycin is represented as a 'C' shape in accordance with observed crystal structure.[58,59]

Acknowledgment. We thank Ilya Koltover, Franck Artzner, and Pradeep Singh for helpful and generous discussions. This material is based upon work supported by the Cystic Fibrosis Foundation, the National Science Foundation via Grants No. DMR08-04363, CBET08-27293, and the RPI-UIUC NSEC. Portions of this research were carried out at the Stanford Synchrotron Radiation Laboratory (SSRL), at the Advanced Photon Source (APS), and at the Fredrick Seitz Materials Research Laboratory (FS-MRL; Urbana, IL). The SSRL Structural Molecular Biology Program is supported by the DOE, Office of Biological and Environmental Research, and by the National Institutes of Health, National Center for Research Resources, Biomedical Technology Program. Use of the APS is supported by the DOE, Office of Basic Energy Sciences, under Contract No. W-31-109-ENG-38.

JA803925N